Perturbation theory of the electronic properties in strongly correlated solids

M. M. Steiner
Theoretical Division MS-B262, Los Alamos National Laboratory, Los Alamos, New Mexico 87545
and Department of Physics B-019, University of California, San Diego, La Jolla, California 92093

R. C. Albers
Theoretical Division MS-B262, Los Alamos National Laboratory, Los Alamos, New Mexico 87545

D. J. Scalapino
Department of Physics, University of California, Santa Barbara, California 93106

L. J. Sham
Department of Physics B-019, University of California, San Diego, La Jolla, California 92093
(Received June, 1990)

In an attempt to obtain a better description than the local-density approximation (LDA) for the electronic structure of realistic narrow-band systems, we have studied a perturbation-theory method for the self-energy and have tested it on the electronic properties of the periodic one-dimensional Anderson model. For a number of models we have calculated a wide range of properties such as quasiparticle energies, spectral densities, reduced hybridizations, and various magnetic correlation functions. For two different models we were able to compare with Monte Carlo results and found good agreement. In general, we have obtained a description of narrow-band systems that is more reasonable than the one given by the LDA.

I. INTRODUCTION

The aim of this study is to incorporate the strong electron-electron correlations inherent in narrow-band materials into *a priori* electronic structure calculations for real solids. Density-functional theory,[1,2] whether in the local-density approximation (LDA) or in the local-spin-density approximation (LSD), has often been successfully used in calculating the ground-state properties and the electronic structure of many systems. In cases where there are discrepancies between calculation and experiment, two questions almost always arise. (1) How good is LDA? (2) How good is the approximation of using the eigenvalues of the Kohn-Sham equation for the band structure? The second point is particularly pertinent since the one-particle Kohn-Sham equation is derived for obtaining the charge density, and its eigenvalues do not therefore need to be the same as the quasiparticle energies.[3] For tetrahedrally bonded semiconductors, the LDA gives a very good exchange-correlation potential.[4] The discrepancy between the LDA band gap and the true gap is because the conduction-band energies are not given by the Kohn-Sham equation. Quasiparticle energies from the Green's function that is constructed from the LDA orbitals are quite satisfactory.[4-6]

For systems with narrow bands, such as the d and f electron series and their oxides, there are physical reasons and computational evidence that both the LDA and the use of density-functional eigenvalues for quasiparticle energies are unsatisfactory; the density-functional eigenvalues do not contain the full quasiparticle renormalization effects that are needed. In the LDA or LSD the exchange and correlation effects of a system are taken locally to be the same as the uniform electron gas with the corresponding density or spin density. This approximation becomes questionable if the conduction or valence electrons are sufficiently localized. Thus, the magnetic properties of these narrow-band systems, such as the spatial distribution of spins from neutron-diffraction experiments,[7] or the temperature dependence of the susceptibility,[8] are often more complex than those derived from the LDA or LSD. While the Fermi surface is remarkably well accounted for by LDA,[9] the LDA d-band width and, therefore, the density-of-states mass can be an order of magnitude off.[10] Also, the energy eigenvalues from LDA cannot explain the spectra from photoemission (PES) and bremstrahlung isochromat spectroscopy (BIS).[11]

A number of schemes have been proposed to augment LDA approaches. For example, to obtain the position of atomic satellites, a LDA total-energy calculation for a supercell in which one site has either one more or one less f electron, together with the total energy for the ground state of the normal number of electrons, gives the position of the $f^n \rightarrow f^{n\pm1}$ peaks.[12] To obtain a heavy mass (large specific heat) in the heavy-electron compounds, renormalized band theory[13] incorporates model resonance f-level behavior into band-structure calculations.

Our ultimate aim is to incorporate the most important narrow-band correlation effects that are included in

such models as the periodic Anderson[14] and Hubbard[15] models into a band calculation for real solids. A successful test would be the ability to account for the magnetic properties, the narrow f-band density of states, and to explain PES-BIS spectra. In this paper we focus on the one-dimensional symmetric and asymmetric periodic Anderson models. Our approach is to use a form of perturbation theory to reproduce the important features of the narrow-band correlations. Using this approach, we hope to test its validity as well as to eventually apply this same method to the full set of orbitals generated by the LDA for a real solid.

The two-band periodic Anderson model is a simplified parametric description of a conduction band (which we will call the d band) interacting with a periodic lattice of localized atomic states (which we will call the f states). The conduction band is characterized by its dispersion relationship, e_k, and its mixing to the localized states through the hybridization V. The energy of the bare localized states is at e_f with respect to the center of the conduction band. Because the f states are spatially compact, strong electron-electron interactions (parameterized by U) are expected between electrons that occupy f orbitals on the same site. Because the Pauli exclusion principle does not allow an electron of the same spin to occupy the same f orbital, this interaction correlates the occupation of the f orbitals of different spins on the same site. Besides these parameters, both the filling and the temperature play important roles in determining the physical properties of the system. We do not study temperature effects here, however.

A LDA approach for this model accounts for the effect of U as a mean-field Coulomb term. In a perturbation theory expansion in U, it thus includes the lowest-order (first-order) term. To improve the LDA theory, it is therefore necessary to take into account at least the second-order terms in U. However, because U can often be the largest energy in the systems of interest, such a straightforward expansion in U would not be expected to be a suitable approach. From another point of view, the mean-field approach of the LDA gives us a static picture, where each orbital is occupied by an average number of electrons $\langle n \rangle$. However, the true instantaneous occupation of an orbital fluctuates around its average value, and is dependent on the instantaneous occupation of the other orbitals. This means that, although $\langle n - \langle n \rangle \rangle$ vanishes, the fluctuations around the mean-field value $\langle (n - \langle n \rangle)^2 \rangle$ do not necessarily vanish. Second order is the lowest order in U that takes this into account. Since the fluctuations might be small even for very large U, there is hope that the range of applicability for an expansion in the fluctuations around the mean-field solution will be larger than that for a direct perturbative approach. For the single-impurity case, Horvatic and Zlatic[16] showed that this approach produces results in good agreement with exact Bethe ansatz results over a large parameter range.

In an attempt to keep track of the many different levels of approximations that we refer to, we will use the following terminology: a "mean-field" solution will refer to the Hartree-Fock solution of the model, i.e., a self-consistent solution to first order in U. Second-order perturbation theory results will refer to the normal expansion of all quantities to second order in U. The method that we use in this paper, i.e., second-order perturbation theory in the fluctuations around the mean-field result, will be called "fluctuation" results, "second-order fluctuations," or more simply "our method." The results that would be obtained if one could exactly solve the model Hamiltonian will be called the "fully interacting" results.

The organization of the rest of the paper is as follows: in the rest of this section we very briefly summarize previously published work that uses this form of perturbative approach to solve the one-dimensional two-band periodic Anderson model. In the next section we present the approach in more detail and formulate how we obtain the observables used to characterize our results. For clarity, some of the details of the calculation are presented in Appendices A and B instead of in this section. In the following three sections we present our results for the symmetric case with some asymmetric cases. We also compare our results, first, to exact Monte Carlo results, whenever possible, and, second, with the mean-field, i.e, LDA, results. Finally, we discuss these results and conclude.

Quite a few different peturbative approaches have been applied to the periodic Anderson model, each making a different set of approximations, and thereby limiting its applicability in the large space of characterizing parameters. Yamada and Yosida[17] have presented the second-order perturbation theory expansion in U around the Hartree-Fock (or mean-field) solution of the symmetric periodic Anderson model. Not much numerical work has been done to follow up on this paper, most probably because of the large computational effort required. Zlatic *et al.*[18] considered the case of interatomic hybridization, within the constant density of states and local approximations. Both Zlatic *et al.* [19] and Okada *et al.* [20] stress the importance of the underlying, unperturbed, mean-field band structure in determining the properties of the perturbed system. Schweitzer and Czycholl[21,22] have looked at the temperature dependence of the f spectral function. Blankenbecler *et al.*[23] compared results of Monte Carlo calculations with second-order perturbation theory results, obtained by using both U and V, respectively, as expansion parameters (the latter is expected to be a good approach for large U). They varied U from 0 to about slightly more than the conduction-band width, and found that the Monte Carlo results crossed over smoothly from the small-U expansion to the small-V expansion. One of the main results of this paper is that this smooth crossover can also be achieved by using the second-order fluctuation theory result for the self-energy.

II. MODEL

The Hamiltonian for the degenerate two-band periodic Anderson model is

$$H = \sum_{k,\sigma} \epsilon_k \; c^\dagger_{k\sigma} c_{k\sigma} + \sum_{i,\sigma} e_f \; f^\dagger_{i\sigma} f_{i\sigma} + V \sum_{k,i,\sigma} \left(e^{ikR_i} f^\dagger_{i\sigma} c_{k\sigma} + e^{-ikR_i} c^\dagger_{k\sigma} f_{i\sigma} \right) + U \sum_i f^\dagger_{i\uparrow} f_{i\uparrow} f^\dagger_{i\downarrow} f_{i\downarrow}, \quad (1)$$

where the first term describes the unhybridized conduction band (the "d band"), and the second term describes a periodic lattice of localized states (the "f states"), which have a bare atomic energy e_f. The third term represents the hybridization between the conduction band and the localized states, and the last term describes the intra-atomic electron-electron interaction between the localized f electrons of different spin. In this paper we use a simple nearest-neighbor tight-binding model for the conduction-band dispersion (ϵ_k); we choose our energy scale so that the center of this unhybridized conduction band is at zero. We also assume no direct f-f hopping, and purely on-site hybridization. These choices are made for simplicity and clarity; generalizations of any or all of these assumptions can be made with relative ease. Although we have examined a range of different parameters, most of the results presented in this paper have $V = 0.375, e_k = -\cos(k)$, in order to be able to directly compare them with existing Monte Carlo results.[23] All energies are in units of $2t$, where t is the d-d nearest-neighbor tight-binding hopping parameter.

In order to expand around the mean-field solution, we follow Yamada and Yosida[17] and also add and subtract the Hartree-Fock term $U(n_f^0/2) f^\dagger_{i\sigma} f_{i\sigma}$, where n_f^0 is the average number of f electrons in the self-consistent ground state of H_0 (see below) at a given filling. We can then separate out a purely one-electron self-consistent or mean-field part of the Hamiltonian H_0 with

$$H_0(U) = \sum_{k,\sigma} \epsilon_k \; c^\dagger_{k\sigma} c_{k\sigma} + \sum_{i,\sigma} \tilde{e}_f \; n_{i\sigma} + V \sum_{k,i,\sigma} \left(e^{ikR_i} f^\dagger_{i\sigma} c_{k\sigma} + e^{-ikR_i} c^\dagger_{k\sigma} f_{i\sigma} \right), \quad (2)$$

where the U dependence enters via the Hartree-Fock atomic energy, $\tilde{e}_f = e_f + U(n_f^0/2)$. Diagonalizing H_0 then yields the eigenvalues

$$e_k^\pm = \frac{1}{2}[\epsilon_k + \tilde{e}_f \pm \sqrt{(\epsilon_k - \tilde{e}_f)^2 + 4V^2}\,] , \quad (3)$$

and the f weight at these solutions is given by

$$\alpha_k^\pm = \frac{1}{2} \left(1 \pm \frac{\epsilon_k - \tilde{e}_f}{\sqrt{(\epsilon_k - \tilde{e}_f)^2 + 4V^2}} \right) . \quad (4)$$

As mentioned in the Introduction, in a more complete calculation of a real solid the self-consistent Hamiltonian H_0 would describe the one-electron bands of a self-consistent LDA calculation. Our H_0 is consistent with this, since the LDA also has an effective mean field $\tilde{e}_f$. We emphasize here that only $\tilde{e}_f$ is present in the mean-field Hamiltonian, and the bare e_f does not therefore enter into the calculation; this point is especially important for the asymmetric case.

The remaining part of the term $U \sum_i f^\dagger_{i\uparrow} f_{i\uparrow} f^\dagger_{i\downarrow} f_{i\downarrow}$ in Eq. (1), which includes to lowest order the fluctuations around the mean-field solution, is treated in perturbation theory up to second order in the self-energy using the Green's-function formalism. In a matrix representation, with the nonhybridized d and f states as a basis, the one-electron retarded zero-temperature Green's function is given by the solution to

$$[\tilde{\omega} - \mathbf{H_0} - \mathbf{\Sigma}_k(\tilde{\omega})] \; \mathbf{G}_k(\tilde{\omega}) \; = \; 1 \; , \quad (5)$$

with $\tilde{\omega} = \omega + \mu + i\delta$, where ω is the energy dependence, μ is the chemical potential, and δ is a positive infinitesimal to give the proper boundary conditions for a retarded Green's function. The fluctuation effects are included in the self-energy $\mathbf{\Sigma}_k$. Because we are only considering on-site f-f correlations, the only nonvanishing element of the self-energy is Σ_k^{ff}. We use a similar form for Σ_k^{ff} as Horvatic and Zlatic used for the single-impurity Anderson model, where it produced good agreement with Bethe-ansatz results[16] (the difference is discussed in Sec. IV). This form is

$$\mathbf{\Sigma}_k^{ff}(\omega) = \frac{U}{2}(< n_f > - n_f^0) \; + \; \Sigma_k^{(2)\,ff}(\omega) \; , \quad (6)$$

with $\langle n_f \rangle$ as the average numbers of f electrons in the fluctuating state. The linear term in U can be considered to be a correction to the mean-field f energy, and is necessary, since the average number of f electrons in the fluctuating state is not always equal to the mean-field solution for the number of f electrons n_f^0. The dynamic correlations are dealt with in the second-order term $\Sigma_k^{(2)ff}$. Details of the form of $\Sigma_k^{(2)ff}(\omega)$, and how it is calculated, are presented in Appendix A.

Information on the one-electron quasiparticles can be obtained from the solution to the Green's function, Eq. (5). The quasiparticles of a LDA calculation are usually assumed to have energies approximated by the one-electron energy eigenvalues of the mean-field self-consistent Hamiltonian and to have infinite lifetimes. The corresponding quantities in the Green's-function formalism are determined by the poles of the Green's function, i.e., the roots of the denominator of the Green's function. In contrast to the band-structure eigenvalues, these roots do not always correspond to zero-width, unit-weight quasiparticles. We determine their weights and widths by analogy to the case where the quasiparticle contribution to the Green's function can be written as a sum of weighted Lorentzian-type poles. In this case, which holds when the poles are not too far from the real axis, we can determine their lifetimes and weights from the imaginary part and the derivative of the real part of the Green's function, respectively. Another approach for finding quasiparticles is to look for peaks in the k-dependent spectral weight. For the mean-field sys-

tem both approaches give identical results; however, for the fluctuating system we will see that this is no longer the case. The f- and d-projected density of states are obtained from the imaginary part of the diagonal elements of the Green's function, i.e., from $\mathrm{Im}G^{dd}(\omega)$ and Im $G^{ff}(\omega)$, respectively, see Eqs. (A2) and (A3).

In strongly correlated systems such as heavy-fermion systems, the large observed specific heats are usually attributed to large effective masses of the quasiparticles. In renormalized band theory this effect is usually built into the theory by reducing the effective f-d hybridization, V, which also reduces the f-d charge fluctuations. To look for this effect in Monte Carlo simulations, Blankenbecler *et al.*[23] examined a normalized effective hybridization defined by $\langle f^\dagger_{i\sigma} c_{i\sigma}\rangle / \langle f^\dagger_{i\sigma} c_{i\sigma}\rangle_0$, which is a measure of the f-d charge fluctuations. This same quantity can be calculated in the Green's-function's formalism. The numerator can be determined from Eq. (A4):

$$\langle f^\dagger_{i\sigma} c_{i\sigma}\rangle = \frac{1}{N\pi}\sum_k \int_{-\infty}^{\mu} d\omega\ \mathrm{Im}G^{df}_k(\omega)\ , \tag{7}$$

$$E^{(2)} = \frac{2}{N}\sum_{k,s} e^s_k f^s_k - U\frac{n^0_f\langle n_f\rangle_0}{4} - \left(\frac{U}{N}\right)^2 \sum_{\substack{k_1,k_2,k_3,k_4,K \\ s_1,s_2,s_3,s_4}} \frac{\alpha^{s_1}_{k_1}\alpha^{s_2}_{k_2}\alpha^{s_3}_{k_3}\alpha^{s_4}_{k_4}}{e^{s_4}_{k_4} - e^{s_1}_{k_1} - e^{s_2}_{k_2} + e^{s_3}_{k_3}}$$
$$\times f^{s_1}_{k_1} f^{s_2}_{k_2}(1-f^{s_3}_{k_3})(1-f^{s_4}_{k_4})\delta(K + k_4 - k_1 - k_2 + k_3), \tag{8}$$

where $\langle n_f\rangle_0$ is the number of f electrons when the mean-field band structure is filled up to the chemical potential of the the fluctuating system, μ, which is chosen so as to give the same total number of electrons in the fluctuating system as there are in the original self-consistent system. (In general, μ and the chemical potential of the mean-field system are different, so that n^0_f and $\langle n_f\rangle_0$ are also different. This means that $\langle n_f\rangle_0$ and $\tilde{e}_f$ are not consistent with one another, which does not worry us, since $\langle n_f\rangle_0$ arises from an intermediate setup.) The linear term is necessary to avoid double counting the Hartree-Fock term. We can also calculate the total energy as the sum of the kinetic, $\langle \mathbf{T}\rangle$, and potential, $\langle \mathbf{V}\rangle$, parts. Using the equation of motion of the destruction operator, $f_{i\sigma}$, we can write the potential energy as[24]

$$\langle \mathbf{V}\rangle = -\frac{i}{2N}\sum_{k,\sigma} \mathrm{Tr}\left[\left(i\frac{\partial}{\partial t} - \mathbf{T}_k\right)\mathbf{G}_k(t,t^+)\right]$$

which, after the Fourier transform, gives for the total energy

$$E = \langle \mathbf{T}\rangle + \langle \mathbf{V}\rangle = \frac{1}{2N\pi}\sum_{k,\sigma}\int_{-\infty}^{\mu} \mathrm{Tr}\left[(\omega + \mathbf{T}_k)\ \mathrm{Im}\mathbf{G}_k\right]\ . \tag{9}$$

To determine the kinetic energy, we calculate the expectation value of the one-particle Hamiltonian, H_0, and subtract off the full Hartree-Fock term. So

$$\langle \mathbf{T}\rangle = \frac{1}{N\pi}\sum_{k,\sigma}\int_{-\infty}^{\mu} \mathrm{Tr}(\mathbf{H}_{0,k}\ \mathrm{Im}\ \mathbf{G}_k) - U\frac{n^0_f}{2}\langle n_f\rangle\ .$$

Putting this into Eq. (9) gives for the total energy

$$E = \frac{1}{2N\pi}\sum_{k,\sigma}\int_{-\infty}^{\mu} \mathrm{Tr}[(\omega + \mathbf{H}_{0,k})\ \mathrm{Im}\ \mathbf{G}_k] - U\frac{n^0_f}{4}\langle n_f\rangle\ . \tag{10}$$

The difference between E and $E^{(2)}$ corresponds to determining the Green's function by summing the infinite series implied in Dyson's equation, $\mathbf{G} = \mathbf{G}_0 + \mathbf{G}_0\mathbf{\Sigma}\mathbf{G}$, rather than simply determining it up to second order, $\mathbf{G} = \mathbf{G}_0 + \mathbf{G}_0\mathbf{\Sigma}\mathbf{G}_0$.

We can also determine various magnetic correlation functions. The square of the f-orbital longitudinal on-site magnetization is

$$\langle (m^f_z)^2\rangle = \langle n_f\rangle - 2\langle n^f_\uparrow n^f_\downarrow\rangle \tag{11}$$

($m^f_z = n^f_\uparrow - n^f_\downarrow$). This can be used as a measure for how strongly correlated the system is, i.e., how strongly the f_σ occupation depends on the $f_{\bar{\sigma}}$ occupation. For an uncorrelated (mean-field) system, $\langle n^f_\uparrow n^f_\downarrow\rangle = \langle n_f\rangle^2/4$, while for a fully correlated system (i.e., for fully spin-polarized solutions, or any linear combination of them such as the

and the denominator is just the same expression, except that the mean-field Green's function is used. In this and all other equations we assume that our one-dimensional system has N sites with periodic-boundary conditions.

The LDA approximation is based on minimizing the total energy with respect to the charge density, and so it is designed to do a good job for calculations of the total energy. According to LDA the total energy of the periodic Anderson model would be the first two terms of Eq. (8) plus the exchange-correlation energy. We assume that LDA treats the exchange part sufficiently well, and therefore consider it to be absorbed into the one-electron parameters in H_0, which means it is part of the first term in Eq. (8). The LDA, however, does not account for the dynamic short-range correlations, which produce the quadratic term in Eq. (8). So, although the LDA should produce the correct U dependence of the total energy for small U, it is expected to be in disagreement with the second-order total energy for large U. The second-order perturbation-theory expression for the total energy per site is

paramagnetic combination) $n_\uparrow^f n_\downarrow^f|\Psi\rangle = 0$. Blankenbecler *et al.*[23] showed that $\langle n_\uparrow^f n_\downarrow^f\rangle$ can be determined from the Hellman-Feynman identity as

$$\frac{\partial\langle H\rangle}{\partial U} = \langle n_\uparrow^f n_\downarrow^f\rangle + \langle n_f\rangle\frac{\partial e_f}{\partial U} . \tag{12}$$

We can also obtain $\langle n_\uparrow^f n_\downarrow^f\rangle$ as $\langle \mathbf{V}\rangle/U$, since $\langle \mathbf{V}\rangle = U\langle n_\uparrow^f n_\downarrow^f\rangle$. Although this produces nearly the same results for large U, it tends to diverge for small U. Generally, for large U, $\langle (m_z^f)^2\rangle$ is 2–5 % larger when determined by this method rather than by using the Hellman-Feynman identity. From linear-response theory we can also determine the remaining magnetic correlation functions, for example, the nearest-neighbor f-d correlation $\langle m_z^f m_z^d(\mathrm{NN})\rangle$. For details of how this is done, see Appendix B.

III. SYMMETRIC CASE

The best studied and simplest case of the one-dimensional two-band periodic Anderson models is the symmetric case. In this case $\tilde{e}_f = \mu = 0$ and the bare f energy is $e_f = \tilde{e}_f - Un_f^0/2 = -Un_f^0/2$. These parameters in the mean-field Hamiltonian, see Eq. (2), are chosen so that there is electron-hole symmetry, i.e., the excitation energy for two f holes or two f electrons on the same site is $U/2$ (the ground state has one f electron per site). We study the U dependence of the symmetric case by varying U from 0 to 4. As mentioned previously, all energies are scaled by $2t$, so that the range of the electron-electron interactions includes a range of systems from those that are weakly correlated to those where U is the largest energy in the Hamiltonian. Note that the bare f energy e_f scales with U so that all symmetric case results presented as a function of U are for systems with different values of e_f as well.

The symmetric case with on-site hybridization has two special properties. First, the mean-field system is an insulator, and, because of Luttinger's sum rule, it remains an insulator for all U. [Luttinger's sum rule states that the number of states enclosed by the Fermi surface of the one-electron Hamiltonian, $\mathbf{H}_{0,k} + \mathbf{\Sigma}_k(\mu)$, is equal to the number of electrons in the perturbed system.[25]] Secondly, because of the symmetry imposed on the system, the d and f occupation numbers are U independent and equal to unity. Thus, for all U, $e_f = -U/2$ and $\langle n_f\rangle = n_f^0 = 1$, and hence the linear term in the self-energy vanishes.

We start by comparing the quasiparticle structure of the mean-field system with that of a system with a substantial U, once the second-order fluctuations have been taken into account. In the center frame of Fig. 1 the solid lines are the U-independent hybridized bands of the mean-field Hamiltonian, see Eqs. (2) and (3). They are also the roots of the denominator of G_k^{ff} for $\Sigma = 0$, see Eqs. (A1) and (A2) in Appendix A, and correspond to zero-width, unit-weight quasiparticles. However, this simple picture, where the roots of the denominator of G_k^{ff} coincide with the peaks in the k-dependent spectral function and can be directly associated with quasiparticles, breaks down when we include the fluctuations. Nonetheless, because the starting point is a Fermi liquid, the analyticity of perturbation theory guarantees that the fluctuating state must also be a Fermi liquid. This means that both the electron number and the number of quasiparticles must be conserved when the effects of the self-energy are included.

The symbols in Fig. 1 are the roots of the real part of the denominator of G_k^{ff} for $U = 4$, once the second-order fluctuations have been taken into account. It is clear that we often have more than two roots at a given k point, and that they can have finite lifetimes as well as weights that are substantially less than unity.[26] Figure 1 also clearly demonstrates the possibility of having a peak in $\mathrm{Im}G_k^{ff}$ without having a corresponding root in the real part of the denominator of G_k^{ff}. For $U = 4$ this is the case for $k \sim 3\pi/8$ and $\omega \sim -0.5$. The roots of the real part of the denominator of G_k^{ff} are only a useful guide to the location of the peaks in the $\mathrm{Im}G_k^{ff}$. Also, not all of these roots can be associated with simple quasiparticle excitations; more complicated excitations can also express themselves as roots of the single-particle Green's function. Finally, the two side frames in Fig. 1 are the f- and d-projected density of states.

A careful examination and classification of the roots shows that, although the picture obtained from the roots is complicated, it is in agreement with our expectations for a strongly correlated system. First, nearly dispersionless and predominantly f-type roots are found near $\pm U/2$ with a weight of about 1/2. These roots are the atomic satellites corresponding to $f^1 \rightarrow f^2$ and $f^1 \rightarrow f^0$ excitations. A numerical explanation for the origin of these satellites is that the high-frequency part of the self-energy behaves as $U^2/4\omega$, which, from Eq. (A2), explains the position and weights of the satellites. To explain this form for the self-energy, we first note that the finite band width implies that $\mathrm{Im}\Sigma_k^{ff}$ vanishes outside the energy range of the mean-field bands, and from the

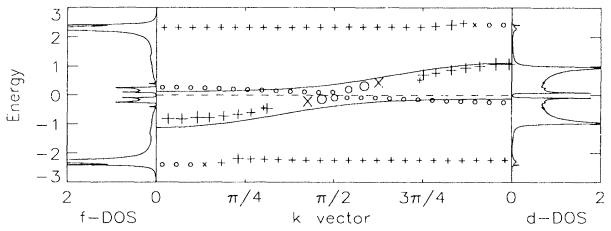

FIG. 1. The roots of the denominator of G_k^{ff} for $U = 4$ for the symmetric periodic Anderson model. In the main part of the figure, the size of the symbols for the roots is proportional to their quasiparticle weight; o, x and + indicate that the widths are less than 0.0133, between 0.0133 and 0.0267, and greater than 0.0267, respectively. The solid line is the hybridized mean-field band structure. The panels on either side of the main part of the figure are the f- and d-projected density of states, which were calculated from the imaginary part of the diagonal f and d Green's functions.

Kramers-Kronig relations that the ω dependence of the high-frequency behavior of the real part is consequently $1/\omega$. For $V = 0$, the numerical factor in the second-order self-energy is $\langle n_f\rangle_0(2-\langle n_f\rangle_0)/4$, which is 1/4 for the symmetric case, and is the same numerical factor obtained for the exact self-energy in this limit. The numerical factor is 1/4 for all two-band one-dimensional symmetric systems. Note that $\langle n_f\rangle_0(2 - \langle n_f\rangle_0)/4$ can be viewed as the total number of possible electron-hole excitations, when a quasiparticle decays into a bare particle and an electron-hole of opposite spin [see Fig. 14(a)]. And finally, from Eq. (A5), we see that the U dependence of the self-energy is U^2. Thus we obtain the $U^2/4\omega$ high-frequency behavior for the large U self-energy that gives the satellites near $\pm U/2$.

Another major set of roots (with approximately unit weights) have predominantly d character and a dispersion very close to $-\cos(k)$, the dispersion of the mean-field d bands. If we characterize the strongly correlated system by only these two sets of roots, we get a picture of a dispersionless f state near $e_f = -U/2$ that is decoupled from a d band with dispersion $-\cos(k)$. An examination of the f- and d-projected spectral weights as U is increased (see Figs. 2 and 3) shows that there is a smooth change in the partial density of states from those of an uncorrelated, hybridized system to those expected for a strongly correlated system, in which the conduction band and the f states are decoupled. This decoupling of the f states from the conduction band can be measured more quantitatively by a reduction in the effective hybridization between the f and d states, see Eq. (7) and Fig. 4. Because the instantaneous occupation of the f orbitals of opposite spin, f_σ and $f_{\bar\sigma}$ orbitals (where $\bar\sigma = -\sigma$), become more strongly correlated upon increasing U, it is expected that the $d_\sigma - f_\sigma$ charge fluctuations will be reduced by the instantaneous $f_{\bar\sigma}$ occupations, producing the observed reduction in the effective hybridization.

Finally, we consider the the nearly dispersionless set of roots, lying just above the chemical potential, near the zone center, and below it, near the zone edge. They have a weight considerably less than unity and also have zero width, see Appendix C. On increasing U they have evolved continuously from the predominantly f-type parts of the hybridized bands, and should therefore be considered as the quasiparticles associated with the atomic satellites. With this in mind, and remembering that $\langle n_f\rangle = 1$, it is natural to associate them with a many-body Kondo (Abrikosov-Suhl) type of resonance. These quasiparticles are responsible for the low-temperature behaviors of the system such as the specific heat, the "coherence temperature," and the Kondo temperature.

As mentioned in the Introduction, renormalized band theory has been used to obtain bands that correctly reproduce the low-temperature properties of Kondo-type materials[13]. In order to compare our results with these types of theory, we have performed a least-squares tight-binding fit to the low-lying excitations. If, in doing this, we fix the d-d nearest-neighbor hopping matrix element (t) and $\tilde e_f$ and only vary V, we obtain a poor fit. In that case we also find that $V^{\rm fit}$ is independent of U, which is out of line with the reduction in the effective hybridization. However, because the self-energy near the chemical potential is strongly k dependent, and has the form[21] $\Sigma_k^{ff}(\omega) \approx A\omega + B\cos(k)$ (where A and B scale as U^2), Eq. (A2) suggests that the most suitable additional parameter to use in the fit would be $t_f^{\rm fit}$, an effective f-f hopping. When this is done, the U dependence of $V^{\rm fit}/V$ and that of the normalized effective hybridization, as determined by Eq. (7), are shown in Fig. 4, along with $t_f^{\rm fit}$. This fit reproduces the positions of the quasiparticles very well, and so we conclude that it is possible to choose a simple set of one-particle parameters that will correctly reproduce the low-temperature properties of the interacting system. The choice of parameters should be based on the low-energy part of the self-energy in order to mimic many-body effects, while remaining within a one-electron picture. However, the resulting one-electron

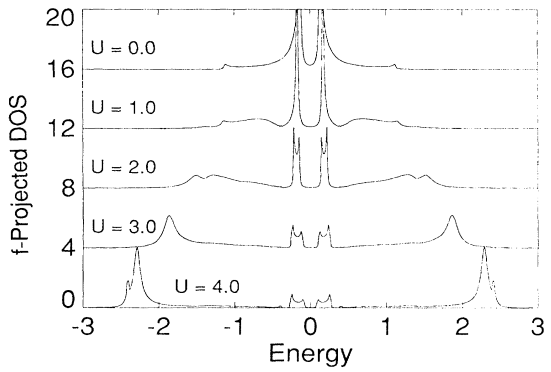

FIG. 2. The energy dependence of the f density of states of the symmetric periodic Anderson model for different values of U. Each curve is offset by four units to keep them from overlapping.

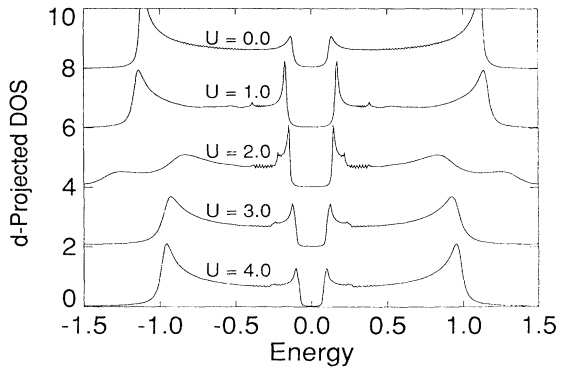

FIG. 3. Same as Fig. 2, except for the d conduction electrons. Note the scale difference. Here, each curve is offset by two units to keep them from overlapping. (The slightly jagged character reflects the discretization of momentum space.)

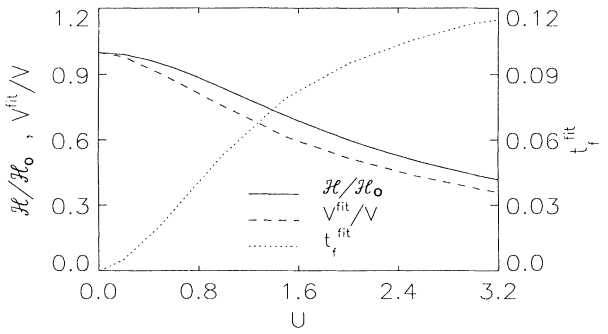

FIG. 4. The normalized effective hybridization ($\mathcal{H}/\mathcal{H}_0$, solid line), the normalized fitted hybridization ($V^{\rm fit}/V$, dashed line), and the fitted nearest-neighbor f-f hopping ($t_f^{\rm fit}$, dotted line), as a function of U for the symmetric periodic Anderson model. The solid and dashed lines use the left-hand scale and the dotted line the right-hand scale. The fitted quantities were determined from tight-binding fits to the low-lying excitations.

bands all have weight equal to unity, which is not in accordance with our results, and also means that the atomic satellites are missing. Luttinger showed that the specific heat depends only on the position of the quasiparticles, not on their weight[27]. So, although the bands obtained from the fitted parameters reproduce the specific heat correctly, their spectral weight will be very different from that obtained from using the complete ω dependence of the self-energy. It should be stressed that the renormalization of the hybridization that we obtain is different from the one obtained using a Gutzwiller variational approach.[28,29] There, the renormalization occurs because double occupancy is projected out, and so, if $\langle n_f \rangle$ is approximately unity, hopping processes are strongly suppressed, which leads to the effective hybridization having the form $V^{\rm eff} = V\sqrt{(1-\langle n_f \rangle)}$. In the symmetric model $\langle n_f \rangle$ is equal to unity for all U, and the origin of the reduction is in the on-site $f_\sigma - f_{\bar\sigma}$ correlations, as discussed above.

By comparing our results to Monte Carlo results, we can test the quality of our approach. In Fig. 5 the Monte Carlo results of Blankenbecler *et al.*[23] for the total energy are reproduced. The Monte Carlo results smoothly cross over from the small-U expansion limit regime, see Eq. (8), to the large-U limit where a small-V expansion is valid. The latter limit, the small-V expansion, which starts with a conduction band as well as flat bands at e_f and $e_f + U$ and then mixes them to lowest nonvanishing order in V, is an extreme example of a strongly correlated system.[23] This expansion is good for small (V/U), and should therefore be valid in the large-U limit. Also shown in Fig. 5 is the total energy as determined from Eq. (10). This follows the Monte Carlo results, and also smoothly crosses over between the two regimes. Good results are obtained for large U because the Green's function has the correct large-U behavior, i.e., it has an atomic satellite at $-U/2$, which occurs for the symmetric case because the second-order fluctuation-theory self-energy has the same high-frequency behavior as the exact self-energy in the V=0 limit (as discussed above). Asymptotically, one obtains an energy of $-U/2$, which is the contribution to the energy of an atomic level at e_f. Half of this energy contribution is the explicit factor of $-U/4$ in the expression for the energy, Eq. (10). A second factor of $-U/4$ comes from the integral over the atomic satellite, which gives a weight of $\sim 1/2$ at the frequency $\sim -U/2$ (a doubling for spin is canceled by a prefactor of 1/2).

As a further corroboration of the validity of our approach, we also compare our results for the square of the local f moment, $\langle (m_z^f)^2 \rangle$, with Monte Carlo results.[23] Figure 6 compares the Monte Carlo results for this quantity with the corresponding results, Eqs. (11) and (12), obtained in second-order perturbation theory in U and V, respectively. We find good agreement in the appropriate limits. As expected, $\langle (m_z^f)^2 \rangle \to 1$, so $\langle n_\uparrow^f n_\downarrow^f \rangle \to 0$ for large U, implying that the instantaneous occupation of the spin-up orbital is strongly correlated with that of

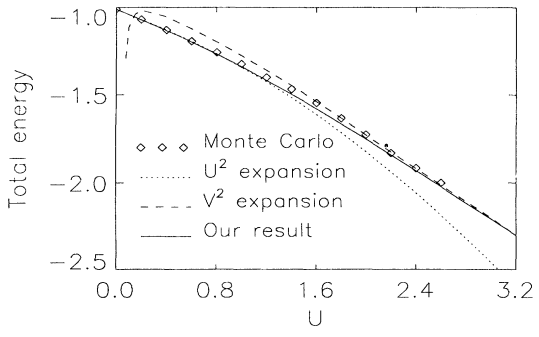

FIG. 5. The total energy as a function of U for the symmetric periodic Anderson model. The solid and dashed lines are the results of second-order perturbation theory in U and V respectively (Ref. 23). The diamonds are Monte Carlo results (Ref. 23), and the dotted line is the second-order fluctuation results, determined by Eq. (10).

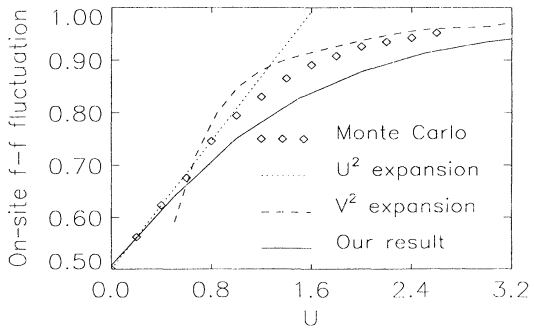

FIG. 6. The on-site square of the f-magnetic moment, $\langle (m_z^f)^2 \rangle$, as a function of U for the symmetric periodic Anderson model. The notation is the same as used in Fig. 5.

the spin-down orbital. So, starting from a static paramagnetic band structure, we obtain a dynamic picture of fluctuating local moments. The spin fluctuations are made possible by the Kondo resonance, which we analyzed above.

IV. ASYMMETRIC CASE I

Although the symmetric case is the most heavily studied limit of the Anderson model, most real systems have neither particle-hole symmetry nor is $\langle n_f \rangle = 1$. In this section we look at the behavior of the asymmetric case in the same fashion as we did for the symmetric case, i.e., by studying its U dependence. In doing this, we will often compare with the simpler symmetric case. There are many ways to break particle-hole symmetry. To make the comparison as tractable as possible, we choose the mean-field parameters to be the same as in the symmetric case, i.e., $\tilde{e}_f = 0$, $V = 0.375$, and with an unhybridized d-band dispersion of $-\cos k$. We introduce the asymmetry by adjusting the chemical potential with U, so that there are always three electrons per unit cell in the fluctuating system. We believe that this form of asymmetry is typical enough to let us make general statements about the validity of our approach for the asymmetric case.

Before looking in detail at the U dependence of the asymmetric periodic Anderson model, we point out some general differences with the symmetric case. First, although the total number of electrons is the same for all U, a redistribution of electrons among the localized and conduction electrons is possible. A direct consequence of this redistribution is that $\langle n_f \rangle$ is not necessarily equal to n_f^0. This means that the f electrons in the fluctuating state experience a different average potential than in the mean-field self-consistent state. The linear term in Eq. (6) accounts for this difference. As previously mentioned, the form of the linear term is slightly different from that of Horvatic and Zlatic. This is because our starting point can be considered a LDA calculation, which yields mean-field instead of bare on-site energies; for the impurity calculation the starting point is the bare on-site f energy. Secondly, for a given U the chemical potential μ and $\delta n_f = n_f^0 - \langle n_f \rangle$ must be determined consistently with $\langle n_f \rangle$ and the total number of electrons. Thirdly, the high-frequency dependence of the second-order part of the self-energy no longer has the simple form $U^2/4\omega$, which resulted in the atomic satellites near $\pm U/2$. Empirically, we find that it typically has the more general form: $[CU^2\langle n_f \rangle_0(2 - \langle n_f \rangle_0)]/[4\ (\omega + \mu - \epsilon_{\text{shift}})]$. Note that $\langle n_f \rangle_0$ is defined, and discussed below Eq. (8). The origin of the filling dependence, $\langle n_f \rangle_0(2 - \langle n_f \rangle_0)$, has been discussed in the previous section. The constant C is a function of V, $\tilde{e}_f$, and μ. It is a factor that accounts for nonzero hybridization and the electron-hole asymmetry; it goes to 1 as $V \to 0$. The ϵ_{shift} term also reflects the electron-hole asymmetry. If $\langle n_f \rangle_0$ is greater than 1, there is a preference for the quasiparticle to decay into a hole, shifting the centroid of $\text{Im}\Sigma_k^{ff}$ to lower

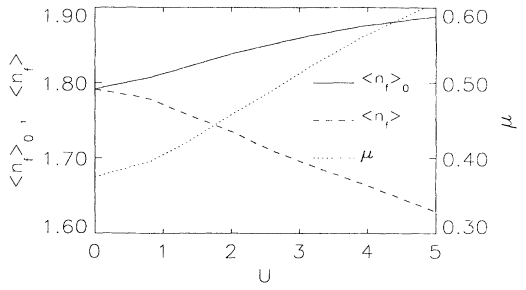

FIG. 7. The number of f electrons in the mean-field bands, using the fluctuating system's chemical potential ($\langle n_f \rangle_0$, solid line, and left-hand scale), and the fluctuation approximation ($\langle n_f \rangle$, dashed line, and left-hand scale), and the chemical potential (dotted line and right-hand scale) as a function of U for the asymmetric periodic Anderson model.

frequencies. So, since $\text{Re}\Sigma_k^{ff(2)}$ is related to $\text{Im}\Sigma_k^{ff}$ by the Kramers-Kronig relationship, the ϵ_{shift} term becomes smaller, which ensures that $\langle n_f \rangle$ is closer to unity than $\langle n_f \rangle_0$. In many cases we have $\epsilon_{\text{shift}} \propto (1 - \langle n_f \rangle_0)$.

Before discussing the quasiparticle structure, we examine the U dependence of the chemical potential, μ, $\langle n_f \rangle_0$, and $\langle n_f \rangle$ (see Fig. 7). As expected, $\langle n_f \rangle$ decreases with increasing U, since double occupation of a localized orbital becomes less favorable. Because of this reduction, $\langle n_d \rangle$ must increase, which, as we will see later, is consistent with the increasing chemical potential as a function of U.

The quasiparticle structure for large U has some similarities as well as some essential differences with the symmetric case. First, it should be mentioned that the Fermi wave vector is equal to $\pi/2$ for all U, in accordance with the prediction of Luttinger's sum rule for a three-electron system. In Fig. 8 we show the roots of the real part of the denominator of G_k^{ff} for the mean-field case and for $U \approx 5.5$. The mean-field bands are the same as in the symmetric case, only the Fermi level has been

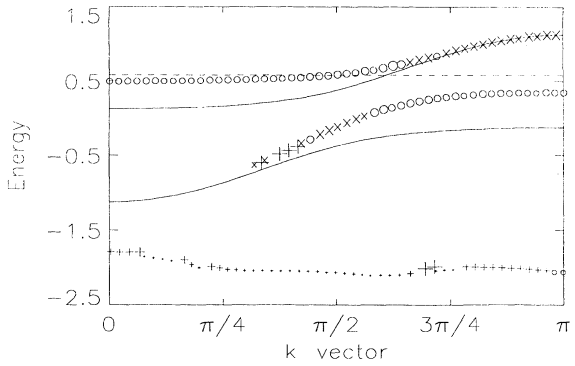

FIG. 8. The roots of the denominator of G_k^{ff} for $U \approx 5.5$. (Same notation as in Fig. 1.)

changed. As for the symmetric model, the $f^1 \rightarrow f^0$ peak separates off from the bottom. However, the $f^1 \rightarrow f^2$ peak is pinned at the Fermi level since $\langle n_f \rangle$ is not near unity. This behavior is typical of a mixed-valence system with more than one f electron per site. It has also been observed by Zlatic *et al.*,[30] using the same approach for the asymmetric single-impurity Anderson model for less than one f electron per site. A partial understanding of this difference from the symmetric case can be found in the form of the high-frequency part of the self-energy for the asymmetric case and from Eq. (A2). Since $\langle n_f \rangle_0$ is nearly U independent, the ϵ_{shift} term is also nearly constant and the constant C depends only very weakly on U via the chemical potential. We define $U^{\text{eff}} = U\sqrt{\langle n_f \rangle_0 (2 - \langle n_f \rangle_0)}$, which is plotted as a function of U in Fig. 11. The reduction relative to U, caused by the change in filling, is considerable. From Eq. (A2), this explains why the separation between $f^1 \rightarrow f^2$ and $f^1 \rightarrow f^0$ peaks is nearly U^{eff} instead of U.

In Figs. 9 and 10 we show the f- and d-spectral weights for various values of U. For $U < 2.5$ (i.e., for $\langle n_f \rangle$ greater than 1.7) we are in the "nearly filled f-orbital" regime, where we expect the behavior to be of the metallic Hartree-Fock type. Thus, we expect the one-electron picture to be valid, with two well-defined quasiparticle bands and very little weight in the satellites. As U is increased, the peaks in the f density of states move up towards the Fermi level. For $U > 2.5$ we enter the mixed valence regime, where the f electrons are pinned to the Fermi level and a localized-state satellite has separated off from the bottom. As we further increase U, the f states are pushed above the Fermi level, thereby reducing $\langle n_f \rangle$; we also find a band forming below the Fermi level, which, away from the Fermi level, is predominantly d type. On further increasing U, the chemical potential rises further, and we recover a filled d band. We never enter a Kondo or heavy-fermion regime, even for very large U, because $\langle n_f \rangle$ never comes close enough to unity

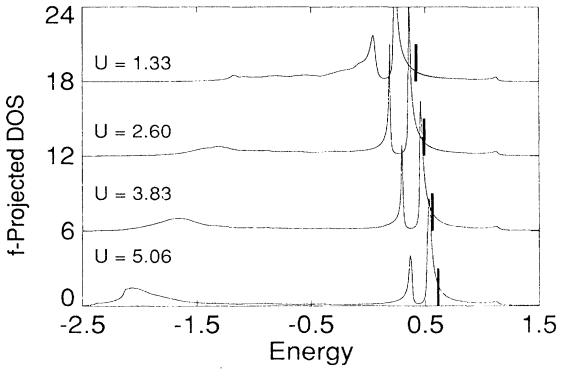

FIG. 9. The energy dependence of the f density of states of the asymmetric periodic Anderson model for different values of U. The perturbed system always has a total of three electrons. The thick vertical lines are the chemical potential in each case. For clarity, each curve is offset vertically by six units.

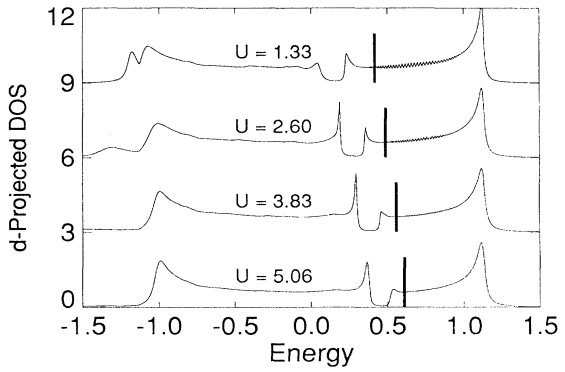

FIG. 10. Same as Fig. 9, except for the d conduction electrons. Note the scale difference. For clarity, each curve is offset vertically by three units. (The slightly jagged character reflects the discretization of momentum space.)

to allow the $f^1 \rightarrow f^2$ peak to form above the top of the d band. This should be contrasted with the symmetric case, where we go directly from a Hartree-Fock insulator to a Kondo-type behavior at $U = 3$, never passing through the mixed-valence state.

From Figs. 8–10 it is clear that the conduction band and the localized states still decouple with increasing U, but not as effectively as in the symmetric case. Again, if we quantify this decoupling by the normalized effective hybridization (see Fig. 11), we find that the U dependence of the effective hybridization is not only much weaker than in the symmetric case, but also slightly increases with increasing U. This increase reflects the redistribution of the three electrons per unit cell among the f and d orbitals, in a fashion that makes f-d charge fluctuations easier. The fact that this redistribution dominates the U dependence of the effective hybridization implies that the $d_\sigma - f_\sigma$ charge fluctuations are only weakly influenced by the instantaneous $f_{\bar{\sigma}}$ occupation, and thus

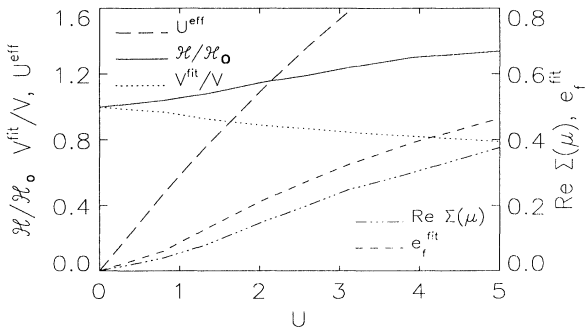

FIG. 11. U^{eff} is plotted against U. The normalized effective hybridization is also compared with the normalized hybridization, obtained from a tight-binding fit. Also Re$\Sigma(\mu)$ and e_f^{fit} are compared.

suggests that the $f_\sigma - f_{\bar{\sigma}}$ correlations are weak, in strong contrast to the symmetric case.

Also shown in Fig. 11 is $\Sigma^{ff}(\mu)$, which is only weakly k dependent. This weak dependence suggests that a tight-binding fit to the low-lying excitations should use $e_f^{\rm fit}$ rather than $t_f^{\rm fit}$ (which was chosen for the symmetric case) and $V^{\rm fit}$, both of which are shown in Fig. 11. There is good agreement between $\Sigma^{ff}(\mu)$ and $e_f^{\rm fit}$, which implies that a renormalization of $\tilde{e}_f$ to $e_f^{\rm fit}$ in Eq. (A2) takes into account the largest part of the self-energy at the Fermi energy, and so explains why $V^{\rm fit}/V$ does not fall off as rapidly as in the symmetric case. The different behavior of $V^{\rm fit}/V$ and the normalized effective hybridization shows that, in general, the dispersion of the low-lying quasiparticles is not a measure of the f-d charge fluctuations over the whole energy range. The fit is very good and again reproduces the low-lying quasiparticle energies very well. The Fermi wave vector and velocity is the same as we obtained from the fluctuation calculation. The quasiparticle bands near the Fermi surface flatten with increasing U, and so increases the effective mass. For example, at $U = 5.06$ there is a threefold increase in the mass. This mass increase occurs because of the renormalization of the effective f level rather than from a decrease in the hybridization. Since these are mixed-valence systems, this is not in contradiction with other renormalized band theories that are applied to Kondo-type and narrow-band systems.

For large values of U, one would expect the U dependence of the second-order total energy, $E^{(2)}$, see Eq. (8), to be dominated by the quadratic term, as in the symmetric case. Surprisingly, however, for large U it is nearly linear, indicating that the Hartree-Fock term is the most important term. The U^2 prefactor is very strongly dependent on the position of the chemical potential. For the transition metals, Friedel and Sayers[31] proposed a simple expression for the prefactor, which, in our case, gives a form proportional to $[\langle n_f\rangle_0(2 - \langle n_f\rangle_0)]^2$. The second-order correction to the total energy in Eq. (8) arises from simultaneously creating up and down spin electron-hole pairs. Neglecting momentum and energy conservation, which is equivalent to the local approximation in the small V limit, we arrive at such a filling dependence for the prefactor. This filling dependence means that it decreases with increasing μ, and thus with U. In actual fact, the reduction more than counteracts the U^2 dependence, and so explains why the second-order contribution to the total energy is small. This is an example of the very strong dependence of the fluctuations on the chemical potential. In this case, the total energy, as obtained from Eq. (10), essentially only differs from the second-order result because of the difference in the form of the Hartree-Fock correction, $Un_f^0\langle n_f\rangle_0/4$ rather than $U\langle n_f\rangle n_f^0/4$.

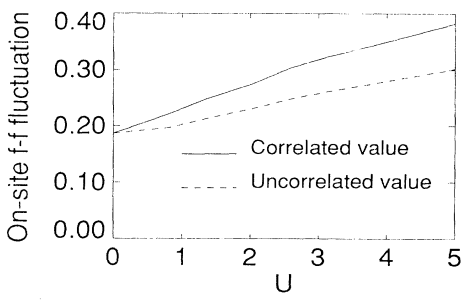

FIG. 12. The on-site $f_\sigma - f_{\bar{\sigma}}$ fluctuations of the perturbed system are compared with the value one would expect for an uncorrelated system with the same f density.

As in the symmetric case, the U^2 expansion overestimates the f-f fluctuations. In Fig. 12 we show the on-site f-f correlation function, determined from E, see Eqs. (10) and (12). The dashed line is $\langle n_f\rangle - \langle n_f\rangle^2/2$, which is the value of $\langle (m_z^f)^2\rangle$ when there are $\langle n_f\rangle$ uncorrelated localized electrons. This implies that, on increasing U, the f electrons remain essentially uncorrelated, even though the three electrons have been redistributed among the f and d orbitals, so as to produce a reduction in $\langle n_f\rangle$. This is in agreement with the conclusions we made for the effective hybridization and total energy.

The three-electron system is the limiting case that separates two classes of systems, namely, those with more (respectively, less) than three electrons. This is because the conduction band can at most be filled with two electrons; so, for a three-electron system, $\langle n_f\rangle$ is never less than unity. Systems with more than three electrons must remain regular Hartree-Fock metals or mixed valence systems for all U. However, for systems with less than three electrons per atom, on increasing U, we can obtain a large variety of possible states, including mixed-valence states, heavy-fermion states, and a system with a partially filled conduction band with a charge-transfer gap to the $f^1 \rightarrow f^2$ peak. To obtain such states continuously from a $U = 0$ state, it is, in general, necessary to vary both $\tilde{e}_f$ and μ with U, so as to fulfill Luttinger's sum rule. However, on going beyond simple model calculations, the parameters are given, and one varies μ so as to obtain the correct total population.

V. ASYMMETRIC CASE II

There are no exact Monte Carlo results for the asymmetric system we discussed above. However, results do exist for the MX systems over a wide range of asymmetry.[32] Examples of MX systems are hypothetical copper-oxide chains and linear halogen-bridged transition-metal chains such as the nickel-bromide chains.[33] The Monte Carlo results of Zotos *et al.*[32] are limited to the population dependence of (a) the number of f electrons in the perturbed system, $\langle n_f\rangle$, and (b) the on-site, nearest-neighbor, and second nearest-neighbor f-f fluctuations. By varying the parameters in the periodic Anderson model, see Eq. (1), it is possible to describe the different regimes of the two-band model, as classified by Zaanen *et al.*[34] By varying the to-

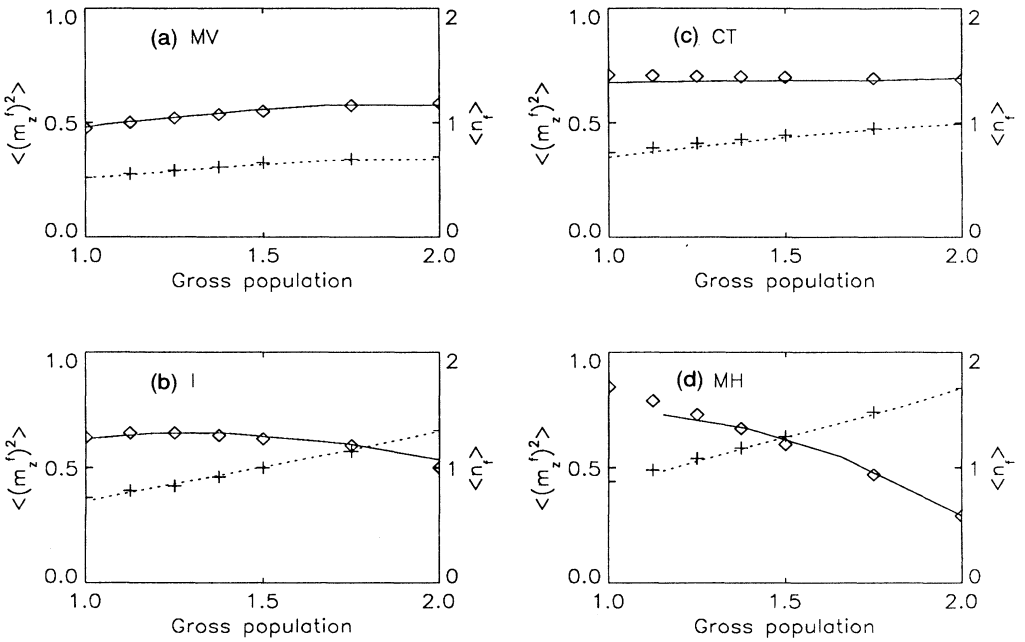

FIG. 13. Comparison of Monte Carlo results with our results for the on-site f-f fluctuations, $\langle (m_z^f)^2 \rangle$, and $\langle n_f \rangle$, for four regimes of the two-band periodic Anderson model: (a) mixed valence, MV; (b) intermediate, I; (c) charge transfer, CT; (d) Mott-Hubbard (MH).

tal filling, the degree of asymmetry may be changed. We mention that for the Anderson model we chose $t = 0.5$, $V = 0.375$, and varied U from 0 to about 5, whereas, for the MX Monte Carlo results, the hopping is the same as the hybridization and is equal to unity. This means that the values of U that are used in the Monte Carlo calculation (i.e., $U = 2$ or 4) should be considered as intermediate, rather than strong, electron-electron interaction strengths.

In Figs. 13(a)–13(d) we compare our results for $\langle n_f \rangle$ and the on-site f-f fluctuations with the Monte Carlo results. Over a large range of electron-hole asymmetry the Monte Carlo results are in good agreement with ours for the three categories: mixed valence (MV), intermediate (I), and charge transfer (CT). Only for the Mott-Hubbard (MH) regime is the agreement less satisfactory, where, for total populations near unity, it is not possible to fulfil Luttinger's sum rule when a reasonably fine energy mesh is used. Thus, on the basis of the overall broad agreement, we believe that it is likely that the results of the previous section would also compare well with exact results.

VI. DISCUSSION AND SUMMARY

The above results suggest various questions, which we will try to answer. First, to what extent have we arrived at a better description of strongly correlated systems than LDA? The results show that we have been successful in including more of the physics that is required to correct the three deficiencies mentioned in the Introduction, viz., the discrepancies between the LDA and the experimental results for the specific heat, magnetic properties, and PES and BIS spectra. We have not been able to compare our results for the effective mass with exact results, so, although we obtain a large mass enhancement, we cannot say whether the U dependence is correct. From Horvatic's and Zlatic's results for the single-impurity case we know that the agreement with exact results for the low-temperature properties is less satisfactory as the asymmetry is increased. All the same, the agreement is still impressive, suggesting a similar approach for the periodic case. As we have seen, starting from a static paramagnetic picture, we have been able to obtain very good agreement with Monte Carlo results for the fluctuating local moment. In the symmetric model, satellites appear near $\pm U/2$, as we expected, whereas in the mixed-valence asymmetric case, only one satellite appeared, which is also to be expected, since we never entered the Kondo regime. It is not clear whether the result that the separation between the $f^1 \rightarrow f^2$ and $f^1 \rightarrow f^0$ peaks is U^{eff} instead of U is purely an artifact of the approach or whether it is correct. The good agreement we get with the exact results for the on-site f-f fluctuations and $\langle n_f \rangle$ implies that the total energy has the correct U dependence, see Eq. (12). This, in turn, indicates that both the near linearity of the total energy, and the high-frequency behavior of the Green's function are correct, see Eq. (10). However, despite the uncertainty about whether we have obtained the correct large-U behavior

for the asymmetric case (because there are no exact results for comparison), the results show that our approach tends to remove some of the worse deficiencies of a LDA approach.

Another question is how does this fluctuation approach compare with exact results? A diagrammatic comparison is made in Appendix D. Wherever comparison has been possible, our results for both the symmetric and asymmetric cases agree well with Monte Carlo results, with the exception of the nearest-neighbor spin correlations where the agreement is only qualitative. As mentioned above, we have not been able to test the quality of our effective-mass results.

A third question is to what extent can one hope to generalize this approach to real systems? The formalism can be easily generalized to three dimensions and many bands (including spin-polarized bands). However, the problem of obtaining the parameters is more complicated. First, to obtain the parameters for the one-electron Hamiltonian it is necessary to subtract off the correlation contribution of the LDA. Secondly, we have to determine the on-site electron-electron interaction, U, in a manner consistent with LDA and our approach. Thirdly, although the largest correlation effects will come from the on-site electron-electron interaction, there are other smaller electron-electron interactions such as d-d, or nearest-neighbor d-f, which could strongly influence Fermi-surface properties and might, therefore, also have to be considered.

It seems possible to determine a simple set of one-electron parameters consistent with the low-lying excitations, while, on the other hand, the separation of the $f^1 \rightarrow f^2$ and $f^1 \rightarrow f^0$ peaks is determined by U^{eff}. This simple picture seems to be an accurate description of our results, whereby, as with all simple pictures, the steps and assumptions made should not be forgotten. We have seen that the form of the self-energy should be used to determine which parameters one should use to describe the bands near the Fermi level. This leads us to pose a final question: is it possible to suggest a parametric form for the self-energy near the Fermi level? We have not been able to find a simple form. Since the linear term of the self-energy has to be determined self consistently with $\langle n_f \rangle$, which can only be determined from a calculation using the full self-energy, to obtain such a form is not a straightforward job.

ACKNOWLEDGMENTS

One of us (M.M.S) was supported by the University of California's Institutional Collaborative Research (INCOR) program for High Temperature Superconductivity. Another (L.J.S) acknowledges partial support by the National Science Foundation under Grant No. DMR-88-15068. Another (D.J.S) wishes to acknowledge support by the Department of Energy under Grant No. DE-FG03-88ER45197.

APPENDIX A

In the nonhybridized basis the Green's function, see Eq. (5), has the form

$$\mathbf{G}_k(\tilde{\omega}) = \begin{pmatrix} G_k^{dd}(\tilde{\omega}) & G_k^{df}(\tilde{\omega}) \\ G_k^{fd}(\tilde{\omega}) & G_k^{ff}(\tilde{\omega}) \end{pmatrix}, \tag{A1}$$

where $\tilde{\omega} = \omega + \mu + i\delta$. On inversion of the bracketed term in Eq. (5) we get, because the only nonvanishing element of the self-energy is Σ_k^{ff},

$$G_k^{ff}(\tilde{\omega}) = \frac{\tilde{\omega} - \epsilon_k}{(\tilde{\omega} - \epsilon_k)[\tilde{\omega} - \tilde{e}_f - \Sigma_k^{ff}(\tilde{\omega})] - V^2}, \tag{A2}$$

$$G_k^{dd}(\tilde{\omega}) = \frac{1}{\tilde{\omega} - \epsilon_k}\left(1 + \frac{|V|^2}{\tilde{\omega} - \epsilon_k} G_k^{ff}(\tilde{\omega})\right), \tag{A3}$$

$$G_k^{df}(\tilde{\omega}) = \frac{V^*}{\tilde{\omega} - \epsilon_k} G_k^{ff}(\tilde{\omega}). \tag{A4}$$

Up to second order in U, we have $\Sigma_k^{ff}(\omega) = \Sigma^{ff\,(1)} + \Sigma_k^{ff\,(2)}(\omega)$, where

$$\Sigma^{ff\,(1)} = \frac{U}{2}(\langle n_f \rangle - n_f^0),$$

and,

$$\Sigma_k^{ff\,(2)}(\tilde{\omega}) = -\left(\frac{U}{N}\right)^2 \sum_{\substack{k_1,k_2,k_3,K \\ s_1,s_2,s_3}} \frac{\alpha_{k_1}^{s_1}\alpha_{k_2}^{s_2}\alpha_{k_3}^{s_3}}{\tilde{\omega} - e_{k_1}^{s_1} - e_{k_2}^{s_2} + e_{k_3}^{s_3}} \times \delta(K + k - k_1 - k_2 + k_3)\left[f_{k_1}^{s_1} f_{k_2}^{s_2}(1 - f_{k_3}^{s_3}) + (1 - f_{k_1}^{s_1})(1 - f_{k_2}^{s_2}) f_{k_3}^{s_3}\right] \tag{A5}$$

with $f_k^s = f(e_k^s)$, and $f(e)$ is the Fermi function. The numerical effort needed to determine $\Sigma_k^{ff(2)}$ can be greatly reduced by reverting to real space, as shown by Treglia *et al.* [35] We rewrite the momentum conserving δ function using

$$\sum_K \delta(K + k - k_1 - k_2 + k_3) = \frac{1}{N}\sum_R e^{i(k - k_1 - k_2 + k_3)R},$$

and defining

$$\rho_R^f(E) = \frac{1}{N}\sum_{k,s} \delta(E - e_k^s)\, e^{ikR}\, \alpha_k^s.$$

We can rewrite Eq. (A5) as

$$\Sigma_k^{ff\,(2)}(\tilde{\omega}) = -\left(\frac{U}{N}\right)^2 \sum_R e^{ikR}\, \Sigma_R^{ff\,(2)}(\tilde{\omega}),$$

with

$$\Sigma_R^{ff(2)}(\tilde{\omega}) = \int de_1 \int de_2 \int de_3 \frac{\rho_R^f(e_1)\rho_R^f(e_2)\rho_R^f(e_3)}{\tilde{\omega} - e_1 - e_2 + e_3} [f_{k_1}^{s_1} f_{k_2}^{s_2}(1 - f_{k_3}^{s_3}) + (1 - f_{k_1}^{s_1})(1 - f_{k_2}^{s_2}) f_{k_3}^{s_3}] \ . \quad \text{(A6)}$$

Numerically it is also favorable to take the limit of vanishing δ, and, after introducing an energy-conserving δ function, to determine the imaginary part of the self-energy. The real part of the self-energy can be determined by the Kramers-Kronig relationship, which converges because of the finite band width. The summation over R is best performed shell-wise; just keeping the $R = 0$ term is called the local approximation.[18] It should also be noted that the self-energy scales as U^2. To determine the Green's functions [Eqs. (A2), (A3), and (A4)], we reintroduce a finite δ of the order of the energy discretization.

APPENDIX B

Using linear-response theory we can also determine the remaining magnetic correlation functions of the fluctuating system. For example, to determine the nearest-neighbor f-d correlation, $\langle m_z^f m_z^d(\mathrm{NN})\rangle$, we introduce two extra terms into the Hamiltonian:

$$U_{\sigma\sigma}^{fd}(\mathrm{NN}) \sum_{i,\sigma} n_{i\sigma}^f n_{i+1,\sigma}^d + U_{\sigma\bar{\sigma}}^{fd}(\mathrm{NN}) \sum_{i,\sigma} n_{i\sigma}^f n_{i+1,\bar{\sigma}}^d \ .$$

We now use Hellman-Feynman and take the derivative of the total energy with respect to $U_{\sigma\sigma}^{fd}(\mathrm{NN})$ and $U_{\sigma\bar{\sigma}}^{fd}(\mathrm{NN})$ to determine $\langle n_\sigma^f n_\sigma^d(\mathrm{NN})\rangle$ and $\langle n_\sigma^f n_{\bar{\sigma}}^d(\mathrm{NN})\rangle$, as a function of the parameters $U_{\sigma\sigma}^{fd}(\mathrm{NN})$ and $U_{\sigma\sigma}^{fd}(\mathrm{NN})$. Taking the limit of $U_{\sigma\sigma}^{fd}(\mathrm{NN}), U_{\sigma\bar{\sigma}}^{fd}(\mathrm{NN}) \to 0$ we are left with only the Hartree and Fock terms, and, finally, taking their difference leaves only the Fock term (coming from the parallel spins). So,

$$\langle m_z^f m_z^d(\mathrm{NN})\rangle = -\frac{2}{N^2} \sum_{k,k'} \cos(k - k') \ n_{\sigma,k}^f n_{\sigma,k'}^f .$$

Similarly, we can get the other magnetic correlation functions.

APPENDIX C

Because we are using a perturbative approach to determine the self-energy, Luttinger's Fermi-surface theorem, which states that at $T = 0$ the quasiparticles at the Fermi surface have an infinite lifetime, always holds. For the symmetric insulator, energy conservation in the determination of the imaginary part of the self-energy [see Eq. (A5)] means that, if there is a root with energy E in the denominator of the real part of G_k^{ff}, such that $|E| < 3\Delta$, where the gap is 2Δ, then $\mathrm{Im}\Sigma_k^{ff} = 0$, and the root will have an infinite lifetime associated with it. Momentum conservation further increases the energy range where $\mathrm{Im}\Sigma_k^{ff}$ vanishes. For the present case a geometrical argument shows that for $E, k > 0$, this range extends from the chemical potential up to $3e^+_{[(k-\pi)/3]}$. These zero-width quasiparticles produce the well-defined low-lying peak(s) in the f-spectral density. From Figs. 2 and 3 it is clear that the gap initially increases with U and then decreases. In light of the decreasing effective hybridization, mentioned above, this behavior is unexpected. The reason lies in the k dependence of the self-energy for small ω. For $U = 0$ there is an indirect gap of 2Δ between the Brillouin-zone center and its edge (see solid lines in Fig. 1). On increasing U, the quasiparticles near the edge and the center move away from the Fermi energy, while those near $k = \pi/2$ move towards it. So, initially, on increasing U, the gap remains indirect and increases, and then becomes nearly direct at $k = \pi/2$, and decreases (see symbols near $k = \pi/2$ and $\omega = 0$). From Fig. 2 we can also see that the existence of the double peak structure discussed by Schweitzer and Czycholl[21] depends on U, or, more exactly, on $U/V^2\rho_0$, where ρ_0 is the DOS of the unhybridized d band.

APPENDIX D

Because we are not using direct perturbation theory in the electron-electron interaction, but rather expanding in the fluctuations around the mean-field solution,

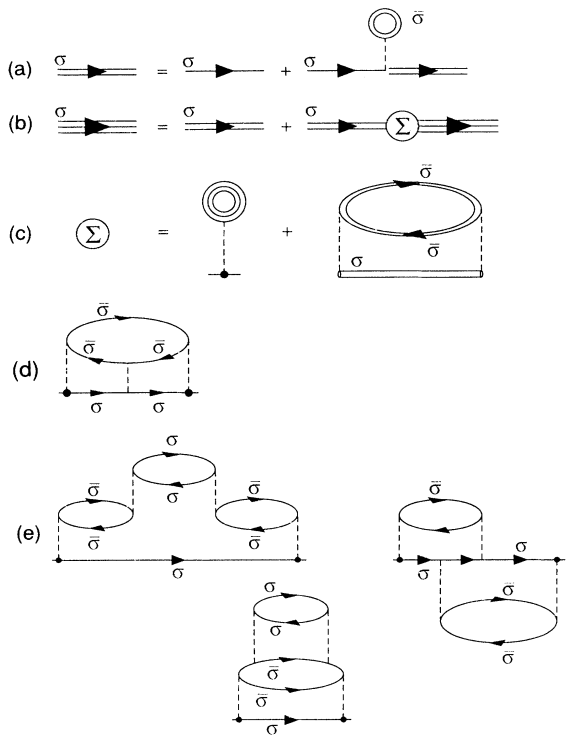

FIG. 14. (a) The self-consistent Green's function (double-lined propagator), (b) the full Green's function (triple-lined propagator), and (c) the self-energy. (d) The missing third-order ladder diagram and (e) the missing fourth-order RPA crossed and stacked diagrams.

a diagrammatic representation is slightly more complicated than usual. First, we have the bare Hamiltonian, i.e, Eq. (1), with $U=0$. The corresponding k- and spin-dependent Green's function is represented by a single line. We represent the self-consistent mean-field Green's function, see Eq. (2), by a double line, see Fig. 14(a). The full Green's function is represented by three lines, and is given by the Dyson equation, see Fig. 14(b). The self-energy consists of two terms, see Fig. 14(c): (i) a self-consistent linear term, which is equal to $U\langle n_f\rangle/2$, and (ii) a second-order term, see Eq. (A5). In Eq. (6) the linear term is $(U/2)(\langle n_f\rangle - n_f^0)$, which only differs from the linear term in Fig. 14(c) in that it has to correct for the mean-field shift already taken into account in $\tilde{\epsilon}_f = \epsilon_f + (U/2)n_f^0$.

By expanding these graphs we can make a comparison to the exact solution. The lowest order in which our approach is different from the exact solution is third order, where we miss the ladder diagram, see Fig. 14(d). For the symmetric case, odd orders vanish, and they are expected to be small for small amounts of asymmetry. For the impurity case this can be deduced from the determinant method.[36] In fourth order we miss the random-phase approximation (RPA), crossed, and stacked diagrams of the types shown in Fig. 14(e). As with any partial summation, one always runs the risk of missing important terms. It is possible to suggest various improvements that would pick up some of the missing terms, such as the inclusion of the RPA series, or self-consistency in the second-order term of the self-energy, as well as in the one-legged series. However, our results agree well with exact results, which indicates that either the terms which we miss are small, or there is a fortuitous cancellation. Yamada has shown that, for the symmetric single-impurity Anderson model, the total proper fourth-order correction is very small, and our approach takes the improper part into account.[37]

[1] P.C. Hohenberg and W. Kohn, Phys. Rev. **136**, B864 (1964).
[2] W. Kohn and L.J. Sham, Phys. Rev. **140**, A1133 (1965).
[3] L.J. Sham and W. Kohn, Phys. Rev. **145**, 561 (1966).
[4] R.W. Godby, M. Schlüter, and L.J. Sham, Phys. Rev. B, **37**, 10 159 (1988).
[5] M.S. Hybertsen and S.G. Louie, Phys. Rev. B **34**, 5390 (1986).
[6] W.E. Pickett and C.S. Wang, Phys. Rev. B **30**, 4719 (1984).
[7] S. Wakoh and J. Yamashita, J. Phys. Soc. Jpn. **35**, 1394 (1973); J.M. Fournier, P.Frings, M. Bonnet, J. Bouscherle, and A. Menousuy, J. Less Common Met. **121**, 249 (1986).
[8] H. R. Ott, in *Progress in Low Temperature Physics*, edited by D.F. Brewer (Elsevier, New York, 1987), Vol. XI.
[9] D.D. Koelling, Solid State Commun. **43**, 247, (1982); W.R. Johanson, G.W. Crabtree, A.S. Edelstein, and O.D. McMaster, J. Magn. Magn. Mater. **31-34**, 377 (1983); M. R. Norman, R. C. Albers, A. M. Boring, and N. E. Christensen, Solid State Commun. **68**, 245 (1988).
[10] See, for example, the review by P.A. Lee, T.M. Rice, J.W. Serene, L.J.Sham, and J.W. Wilkins, Comments Solid State Phys. **12**, 99 (1985).
[11] F.J. Himpsel, J.A. Knapp, and D.E. Eastman, Phys. Rev. B **19** 2919 (1979); A.M. Boring, R.C. Albers, G. Schadler, P. Marksteiner, and P. Weinberger, *ibid.* **35** 2447 (1986); R.C. Albers, A.M. Boring, L.E. Cox, O.R. Eriksson, and N.E. Christensen (unpublished).
[12] M.R. Norman, D.D. Koelling, and A.J Freeman, J. Magn. Magn. Mater. **47-48**, 255 (1985).
[13] P. Fulde, J. Keller, and G. Zwicknagl, Solid State Physics, **41**, 2 (1988).
[14] P.W. Anderson Phys. Rev. **124**, 41 (1961).
[15] J. Hubbard, Proc R. Soc. London Ser. A **276**, 238 (1963); *ibid.* **277**, 237 (1964); *ibid.* **281**, 401 (1964).
[16] B. Horvatic and V.Zlatic, Solid State Commun. **54**, 957 (1985).
[17] K. Yamada and K. Yosida, in *Theory of Heavy Fermions and Valence Fluctuations*, edited by T. Kasuya and T. Saso (Springer, New York, 1985), p.183; in *Electron Correlation and Magnetism in Narrow-Band Systems*, edited by T. Moriya (Springer, New York, 1981), p.210.
[18] V. Zlatic, S.K. Ghatak, and K.H. Bennemann, Phys. Rev. Lett. **57**, 1263 (1986).
[19] V. Zlatic, A.A. Aglia, and D. Schultz, J. Magn. Magn. Mater. **76**, 70 (1988).
[20] K. Okada, K. Yamada, and K. Yosida, Prog. Theor. Phys. **77**, 1297 (1987).
[21] H. Schweitzer and G. Czycholl, Z. Phys. B Condens. Matter **74**, 303 (1989).
[22] H. Schweitzer and G. Czycholl, Solid State Commun. **69**, 171 (1989).
[23] R. Blankenbecler, J.R. Fulco, W. Gill, and D.J.Scalapino, Phys. Rev. Lett. **58**, 411 (1987).
[24] J.W. Negele and H.Orland, *Quantum Many-Particle Physics* (Addison-Wesley, New York, 1988).
[25] R.M. Martin and J. Allen, J. Appl. Phys. **50**, 7561 (1979); R.M. Martin, Phys. Rev. Lett. **48**, 362 (1982).
[26] We do not approximate the self-energy by a constant, such as $\Sigma_k^{ff}(\mu)$, which one does to test Luttinger's sum rule, but keep the full frequency dependence of the self-energy. This means that to obtain the roots we need to find the zeros of an equation, which is more complicated than the simple quadratic case, which we would have had, if we had just used $\Sigma_k^{ff}(\mu)$, see Eq. (A2).
[27] J.M. Luttinger, Phys. Rev. **119**, 1153 (1960).
[28] T.M. Rice and K. Ueda, Phys. Rev. Lett. **55**, 995 (1985).
[29] B.H. Brandow, Phys. Rev. B **33**, 215 (1986).
[30] V. Zlatic, B. Horvatic, and D. Sokcevic, Z. Phys. B Condens. Matter **59**, 151 (1985).
[31] J. Friedel and C.M. Sayers, J. Phys. B (Paris) **38**, 697 (1977).
[32] X. Zotos, W. Lehr, and W. Weber, Z. Phys. B Condens. Matter **74**, 289 (1989).
[33] K. Toriumi, Y. Wada, and T. Mitani, Phys. Rev. Lett. **55**, 995 (1985).
[34] J. Zaanen,G.A. Sawatzky, and J.W. Allen, J. Magn. Magn. Mater. **54-57**, 607 (1986).
[35] G. Treglia, F. Ducastelle and D. Spanjaard, J. Phys. B (Paris) **41**, 281 (1980).
[36] N. Menyhard, Solid State Commun. **12**, 215 (1972).
[37] K. Yamada, Prog. Theor. Phys. **53**, 970 (1975).